Atmos. Chem. Phys., 14, 8579–8597, 2014
www.atmos-chem-phys.net/14/8579/2014/
doi:10.5194/acp-14-8579-2014

Atmospheric Chemistry and Physics
Open Access

A climatology of dust emission events from northern Africa using long-term surface observations

S. M. Cowie[1], P. Knippertz[2], and J. H. Marsham[1]

[1]Institute for Climate and Atmospheric Science, School of Earth and Environment, University of Leeds, Leeds, LS2 9JT, UK
[2]Karlsruher Institute of Technology, Kaiserstr. 12, 76131 Karlsruhe, Germany

Correspondence to: S. M. Cowie (eesc@leeds.ac.uk)

Received: 6 February 2014 – Published in Atmos. Chem. Phys. Discuss.: 18 March 2014
Revised: 25 June 2014 – Accepted: 14 July 2014 – Published: 25 August 2014

Abstract. Long-term (1984–2012) surface observations from 70 stations in the Sahara and Sahel are used to explore the diurnal, seasonal and geographical variations in dust emission events and thresholds. The frequency of dust emission (FDE) is calculated using the present weather codes of SYNOP reports. Thresholds are estimated as the wind speed for which there is a 50 % probability of dust emission and are then used to calculate strong wind frequency (SWF) and dust uplift potential (DUP), where the latter is an estimate of the dust-generating power of winds. Stations are grouped into six coherent geographical areas for more in-depth analysis.

FDE is highest at stations in Sudan and overall peaks in spring north of 23° N. South of this, where stations are directly influenced by the summer monsoon, the annual cycle in FDE is more variable. Thresholds are highest in northern Algeria, lowest in the latitude band 16–21° N and have greatest seasonal variations in the Sahel. Spatial variability in thresholds partly explain spatial variability in frequency of dust emission events on an annual basis. However, seasonal variations in thresholds for the six grouped areas are not the main control on seasonal variations in FDE. This is demonstrated by highly correlated seasonal cycles of FDE and SWF which are not significantly changed by using a fixed, or seasonally varying, threshold. The likely meteorological mechanisms generating these patterns such as low-level jets and haboobs are discussed.

1 Introduction

Northern Africa is firmly established as the biggest contributor of mineral dust into the atmosphere (Prospero, 2002; Goudie and Middleton, 2001). There are large geographical variations across the region with the intensity of a source area depending on surface properties (soil moisture, vegetation, roughness, soil composition and particle size), meteorological parameters (wind, stability), and even on the extent of anthropogenic activity (Ozer, 2001; Mahowald et al., 2002; Ginoux et al., 2012). The Sahara desert contributes more dust to the atmosphere than the semi-arid Sahel, though the Sahel has been proposed to be the main factor in interannual and seasonal variability of dust exports (Zender and Kwon, 2005; Evan et al., 2006). Once airborne, dust particles from northern Africa can be transported for thousands of kilometres and alter climate by scattering, reflecting and absorbing incoming short-wave and outgoing long-wave radiation at both the surface, and the top of the troposphere (Sokolik et al., 2001). Cooling takes place when absorbing and scattering reduces the amount of energy which reaches the surface (Kaufman et al., 2002; Spyrou et al., 2013) while atmospheric warming takes place when aerosols absorb and re-emit outgoing long-wave radiation (Dufresne et al., 2002). Current radiative forcing estimates of mineral dust are highly uncertain, but an overall negative (atmospheric cooling) effect of $0.1(\pm 0.2)\,\mathrm{W\,m^2}$ is predicted (Stocker et al., 2013). Deposited dust particles can not only impact on ocean biogeochemical processes (Mahowald et al., 2005), but also on land ecosystems such as the nutrient-depleted Amazon basin (Bristow et al., 2010).

As the starting point of the global dust cycle, emission is a crucial process. However, current estimates on a regional and even a global scale are highly uncertain. At present, there is no network of observations to sufficiently constrain the global dust budget, so estimates at least partly rely on numerical models (Tegen and Schepanski, 2009). A recent systematic comparison of state-of-the-art global models showed a range in emissions from 400 to 2200 Tg year^{-1} (Huneeus et al., 2011) from North Africa.

Dust emission is a highly non-linear function of wind speed, with the exceedance of a threshold value required to start emission (Helgren and Prospero, 1987; Bagnold, 1941). This threshold is controlled by surface characteristics, which is particularly important in semi-arid areas like the Sahel where the cycle of emission, transport and deposition is complex and intertwined with seasonal rainfall and vegetation. The main impacts here are thought to be through changing seasonal amounts of bare soil surface (Kim et al., 2013) and the effects of varying roughness from vegetation on localised peak winds (Roderick et al., 2007; Vautard et al., 2010; Cowie et al., 2013). Rainfall, and its subsequent impact on soil conditions and surface composition, can enhance or suppress dust emission on diurnal to inter-annual timescales through different mechanisms (Zender and Kwon, 2005). Important to arid and semi-arid areas are the alternate flooding and drying out of ephemeral (temporary) lakes, wadis and alluvial fans (Mahowald et al., 2003; Ginoux et al., 2012). Alluvial fans funnel rainwater from local hills and elevated terrain down into topographic lows where many of the major northern Africa dust sources, as identified by satellite observations, are shown to be located (Prospero, 2002).

Meteorological mechanisms involved in producing dust emission in northern Africa act on synoptic, meso- and micro-scales. Synoptic mechanisms are based around the establishment of a large surface pressure gradient. In the boreal winter this occurs between the Azores High intruding into Morocco, Algeria and Libya and the tropical pressure trough near the Gulf of Guinea. The strong northeasterly winds driven by this pressure difference are known as "harmattan" and are particularly important for dust sources in southern parts of the Sahara and the Sahel in winter (Klose et al., 2010). Driven by the large pressure gradient described above, a wind-speed maximum frequently forms in the lower troposphere, commonly known as a low-level jet (LLJ). LLJs also occur in the southern Sahara and Sahel during summer, when surface pressure gradients around the Saharan heat low (SHL) encourage their formation. Nocturnal low-level jets (NLLJs) are LLJs which develop (or are enhanced) at night-time (Fiedler et al., 2013a). The morning breakdown of a NLLJ by surface heating produces gusty winds which in turn initiate dust emission. LLJs can also occur in the daytime due to baroclinic conditions forced by coastlines and complex terrain (Stensrud, 1996).

Another synoptic-scale mechanism is uplift by the leading edge of the West African summer monsoon flow, which can essentially act as a large density current (Bou Karam et al., 2008) and is often referred to as the intertropical discontinuity (ITD). Variability in the position of the ITD has been linked to variability in dust uplift over West Saharan dust sources (Engelstaedter and Washington, 2007) through associated LLJs (Knippertz, 2008) and haboobs (Marsham et al., 2008). This variability is partly controlled by disturbances that form on the African easterly jet (AEJ), called African easterly waves (AEWs). AEWs can alter the position of the ITD, creating northward excursions of southerly monsoon flow and uplift in the southern Sahara (Marsham et al., 2013). The AEW surface vortex itself can also produce winds strong enough for emission (Knippertz and Todd, 2010). In addition to the leading edge, dust emission has been observed within the moist southwesterly monsoon flow from the Gulf of Guinea. Some evidence suggests that the dominant mechanism is gusty cold-pool outflows from convection (Marsham et al., 2008), though LLJs are also known to be embedded in the monsoonal flow (Parker et al., 2005). Acting on the meso-scale, these gusty cold-pool outflows, or density currents, create large dust storms which can extend to several hundred kilometres. These are commonly referred to as "haboobs". Dust emission due to haboobs has been documented in the northwest Sahara (Knippertz et al., 2007; Emmel et al., 2010), in the Sahel (Sutton, 1925; Williams et al., 2009) and southern Sahara (Knippertz and Todd, 2010; Marsham et al., 2013; Allen et al., 2013). It is difficult to assess the frequency of haboobs due to satellite sensing limitations in cloudy conditions (Heinold et al., 2013; Kocha et al., 2013) and the sparse network of surface observation stations.

Micro-scale dust emission mechanisms take place under strong surface heating and light background winds. These conditions support the formation of rotating dust devils, and longer-lived, non-rotating dust plumes (Koch and Renno, 2005). Due to their small scales it is hard to compile a comprehensive climatology for a large area like northern Africa. Current estimations are based on extrapolating field campaign analysis to a wider area. Recent advances in remote sensing of atmospheric dust from satellites have been invaluable, but are not without limitations such as cloud contamination, assumptions made on optical properties, variability in surface albedo and emissivity over land (Knippertz and Todd, 2012). It is also very hard to separate airborne dust from dust emission in remotely sensed data. Some products are only available daily, making them unsuitable to investigate the large diurnal cycle in dust emission. While routine surface observations can only give point measurements, they do provide long-term records and are not subject to the limitations of satellite data mentioned above. In this paper, we use long-term observations from standard surface weather stations across North Africa which report at 3- and 6-hourly intervals to compile climatological statistics, including the diurnal cycle. Despite the sparse area coverage of northern Africa, these data have a high value for dust emission studies and have been explored surprisingly little in the literature. Up

to now, surface observations of visibility and present weather have been used for statistical analysis in the Sahel and Sahara (Mbourou et al., 1997; Mahowald et al., 2007; Klose et al., 2010), but have not isolated dust emission events specifically. Climatological studies of dust emission, from surface SYNOP present weather reports, have only been conducted for East Asia (Kurosaki and Mikami, 2005), the southwest summer monsoon region (Ackerman and Cox, 1989; Middleton, 1986) and Australia (McTainsh and Pitblado, 1987).The seasonal and diurnal cycles of dust are explored in relation to visibility and rainfall in Mbourou et al. (1997) while Marticorena et al. (2010) discuss dust concentration and strong wind frequency. The time and spatial scales of these two studies are quite different with 53 stations and three 4-year periods investigated in Mbourou et al. (1997) compared to three stations for a 3-year period in Marticorena et al. (2010). This paper intends to build on the information gathered by these studies by including a larger spatial area, a longer data record and new data analysis techniques which aim to clearly separate emission from transport events.

This paper presents a climatology of dust emission events from SYNOP observations from northern Africa, objectively determines wind-speed thresholds for emission and applies new diagnostics and statistics to assess seasonal and diurnal cycles of these events. Section 2 will focus on how dust emission is identified from surface observations, on the criteria and quality flags applied to the station data and on diagnostic tools used for analysis. Section 3 presents the results of the seasonal and diurnal cycle of dust emission, with discussion on individual stations followed by stations grouped together in Sect. 3.2. Changes in emission threshold, both geographically and temporally, will also be discussed in Sect. 3.

2 Data and methods

2.1 Observational data

2.1.1 Routine surface SYNOP observations

Long-term surface observations are recorded as SYNOP reports, which include 3-hourly observations of 10 min mean wind-speed, measured at a height of 10 m by an anemometer, and present weather subjectively judged by a human station observer using a code defined by the World Meteorological Organization (WMO). The present weather (ww) codes describing dust emission are 07–09, 30–35 and 98 (WMO, 1995). These descriptions of dust emission weather do not provide information on the physical processes at a particle scale, but simply describe how the dust appears in the atmosphere to the observer. As in Kurosaki and Mikami (2005), we split these codes into "blowing dust" (07 and 08) and "dust storms" (09, 30–35 and 98), which represent dust events on a larger scale and may also be more intense. Information on visibility is purposely omitted, as the relative contribution of advected and locally emitted dust particles to low visibility is unknown. The code 06 ("dust not raised by wind, at or near the station") is extracted to investigate non-emission dust events. For the purpose of this study we label these events as "transported dust". We transform groups of reports into frequency of occurrence parameters. Frequency of dust emission (FDE) is the percentage of dust events (all emission codes) reported at a given time of day or during a certain month, with respect to the total number of observations. Dust storm frequency (DSF), blowing dust frequency (BDF) and transported dust frequency (TDF) are calculated in the same way, but with the particular codes for dust storms and blowing dust as described above.

SYNOP reports were taken from the Met Office Integrated Data Archive System (MIDAS) data set. As we are primarily interested in dust emission, the first criterion for stations to be selected was for 1060 observations of dust emission over the time period 1984–2012: 70 stations, displayed in Fig. 1, fulfilled this criterion and form the basis of this study. The ratio of day to night-time observations, as well as the number of observations per year, was investigated in order to create a quality flag system for the stations. Quality flags consists of a number (1 or 2) proceeded by a letter (A, B or blank). Where the ratio of day to night observations is greater than 2 : 1 a 2 flag is given, while a 1 is applied to a non-biased station. Healthy stations with more than 500 observations per year for each year between 1984 and 2012 do not have a letter flag. Stations which have less (greater) than 5 years with less than 500 observations per year are marked A (B).

The 29 years of SYNOP data included some wind-speed reports above realistic values; in some cases a typographic error was clear. We analysed some of the strongest winds from the study period with SEVIRI data (2006–2012) and found that the strongest (realistic) wind associated with a dust emission report was a 54 kn report accompanied by a noticeable cold pool outflow in the satellite imagery. Since we could not confirm any of the other reports at greater speeds than this, wind speeds greater than 55 kn were removed from the analysis.

In the Sahel region 6-hourly sampling is more common than 3-hourly sampling. Different sampling regimes tend to be confined to within countries. For example in Mauritania nearly all stations have no night-time observations, while in Mali and Niger sampling tends to be limited to 6-hourly. This is documented in detail in Fig. S1 in the Supplement. Analysis of 6-hourly data was applied to stations which have stable 3-hourly sampling. The magnitude of annual FDE varied at a few stations, but overall the seasonal cycle remained similar at all but one station (Fig. S2 in the Supplement). We suspect that this is due to natural inter-station variability in the diurnal distribution of dust emission mechanisms between SYNOP and inter-SYNOP hours. The approach we take in this paper is to highlight the main biases which might affect conclusions that apply to large areas and groups of stations,

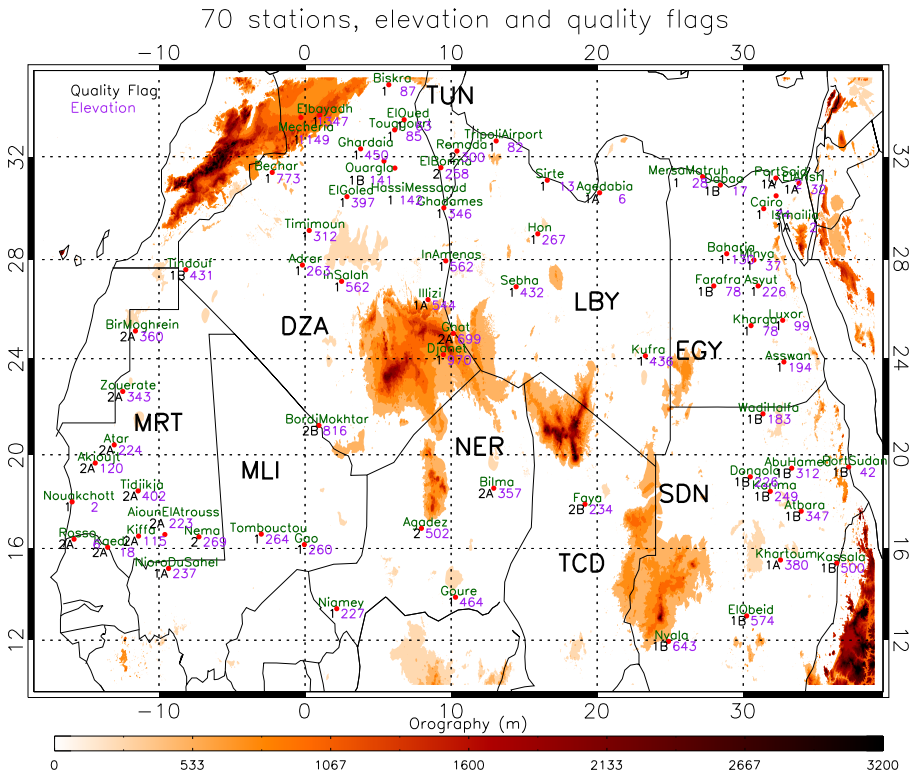

Figure 1. Geographical overview. Map of observation stations used in the study, with quality flags in black (see Sect. 2.1.1) and elevation in purple. Country codes, as defined by ISO (International Organization for Standardization): DZA = Algeria, TUN = Tunisia, MRT = Mauritania, MLI = Mali, NER = Niger, LBY = Libya, EGY = Egypt, TCD = Chad and SDN = Sudan. Colour shading gives the orography in m.

rather than focusing on the effect of individual station biases on their individual results.

Station location, elevation and quality flag values are displayed in Fig. 1. Not surprisingly, SYNOP stations are rare in the interior of the Sahara and more commonly situated on the fringes, where precipitation is abundant enough to sustain vegetation, crops and livestock. The stations in Sudan are all located along the Nile, as are most Egyptian stations. Southern Mauritania and northern Algeria have a relatively good network. The stations of Bordj Mokhtar (southern Algeria) and Faya (northern Chad) are particularly valuable due to their close location to two well-known dust sources. The former was the location of a supersite during the recent Fennec field campaign (Marsham et al., 2013), while the latter is close to field activities during BoDEx (Washington et al., 2006). The elevations of the stations vary from 2 m (Nouakchott and Port Said) to 1347 m at Mecheria in the foothills of the Atlas Mountains in northern Algeria (Fig. 1). The healthiest station records are found in the north, as the distribution of quality flags in Fig. 1 indicates. Civil unrest in Sudan may be the cause of large gaps in the station records, as all stations there have an A or B flag. The central and western Sahel stations are most affected by lack of night-time data and most stations there have a 2 flag. This is a problem for the Sahel region where haboobs commonly occur and are known to uplift dust in the evening and night-time (Marsham et al., 2013).

2.1.2 Satellite observations of normalized difference vegetation index

To better understand temporal variations in emission threshold, the main seasonal cycle of vegetation is investigated, which in the Sahel is primarily constrained by precipitation (Fensholt et al., 2012) and is thought to be a better indicator of soil moisture than rainfall (Nicholson et al., 1990). The normalized difference vegetation index (NDVI; Tucker et al., 2005) is a popular proxy for vegetation, especially in semi-arid areas such as the Sahel (Huber and Fensholt, 2011; Olsson et al., 2005) to which it is particularly well suited. A limitation of this data set is that NDVI only detects green vegetation and may overestimate areas with low Leaf Area Indices (Zhu et al., 2013), such as semi-arid regions. After the main growing season brown vegetation, which still affects dust emission (Zender and Kwon, 2005), is likely to be left over, but not detected by NDVI. NDVI data are accessed from the Global Inventory Modeling and Mapping Studies (GIMMS) database (www.landcover.org), which covers the time period

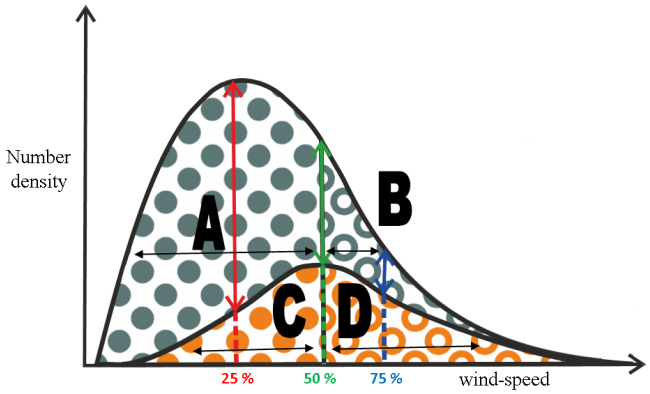

Figure 2. Schematic to illustrate the estimation of emission thresholds. Orange shading indicates the number density function of wind speeds associated with dust emission reports and grey shading represents wind speeds for all observations. The arrows signify the wind speed at which dust emissions make up 25, 50 and 75 % (red, green and blue respectively) of all reports. Areas A and B are represented by grey dots and circles, C and D with orange dots and circles. For a detailed discussion of this schematic, see Sect. 2.2.1.

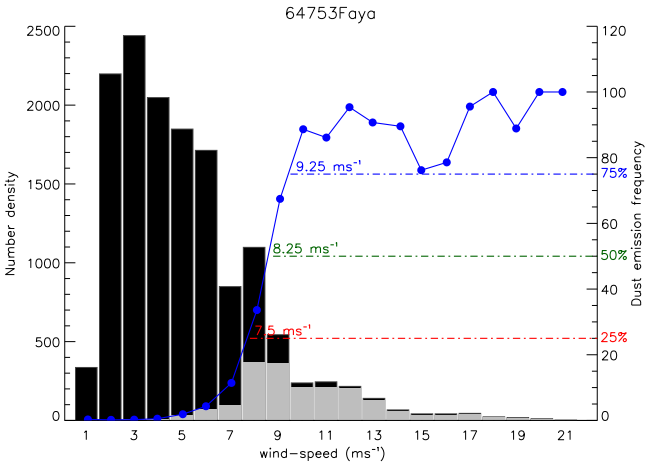

Figure 3. Example wind climatology for Faya (WMO no. 64753) in Chad (see Fig. 1 for location). Number distribution of surface wind speed for the time period 1984–2012. Black bars and grey bars give the distribution of all winds and those associated with dust emission only, respectively. Dust emission frequency ((grey/black) · 100) for each wind-speed bin is given by the blue dots. T25, T50 and T75 threshold values are given in red, green and blue, respectively.

1984–2006 and is calculated for a 24 km by 24 km box over each station location.

2.2 Methods

2.2.1 Analysis of dust emission thresholds from SYNOP data

For any land surface, there is a minimum surface stress that must be exerted by the wind to generate dust emission. This stress closely corresponds to a threshold speed for the low-level wind (Helgren and Prospero, 1987). The threshold wind speed for a surface is determined by the surface roughness and soil properties (such as particle shapes and sizes, soil composition, moisture content and aerodynamic properties) but can also be influenced by previous disturbance of the soils (Gillette et al., 1980). Although we do not have long-term measurements of soil conditions, it is possible to statistically evaluate which wind speeds are most likely to be associated with reported dust emissions.

We use two alternative approaches to measure the relationship between reported dust events and anemometer wind speed. The first method compares the probability density function (PDF) of winds during dust emission events (bottom black curve in Fig. 2) with those considering all reports for a given station (top black curve in Fig. 2, and is based on work by Morales, 1979; Helgren and Prospero, 1987; Kurosaki and Mikami, 2007). Based on these PDFs, the wind speeds at which 25, 50 and 75 % of all observations contain a dust emission report can be computed (herein T25, T50 and T75; see vertical lines in Fig. 2). Within the remainder of the paper we focus on T50, but T25 and T75 are useful to describe the range of observed thresholds. A real-world example from the station of Faya in Chad is shown in Fig. 3. The large majority of observed wind speeds are in the range of 2–6 $\mathrm{m\,s^{-1}}$ (black bars). Dust emission starts around 4 $\mathrm{m\,s^{-1}}$, but remains a small fraction of all observations up to 7 $\mathrm{m\,s^{-1}}$. Beyond this value the dust fraction increases quickly and from 10 $\mathrm{m\,s^{-1}}$ onwards practically all observations contain dust emission reports.

In order to test the relationship between the occurrence of dust emission and the occurrence of strong winds, we define the parameter strong wind frequency (SWF) as the percentage of all wind observations exceeding T50. If the threshold behaviour is well defined (as in Fig. 3), FDE and SWF should behave in a similar way, but this is not generally the case and differences will depend on the exact shapes of the two PDFs. To illustrate the effect, four areas are distinguished in Fig. 2. Area A represents winds below T50 without dust emission, B winds above T50 without dust emission, C winds below T50 with dust emission and D winds above T50 with dust emission. All observations are then $N = \mathrm{A}+\mathrm{B}+\mathrm{C}+\mathrm{D}$. Consequently, Area C+D represents all dust emission events and therefore FDE is the fraction $(\mathrm{C}+\mathrm{D})/N$. SWF is represented by the fraction $(\mathrm{B}+\mathrm{D})/N$. If FDE = SWF then this implies that C = B. Four cases can be distinguished. If both C and B are small, FDE ≈ SWF and the threshold must be sharp. If both C and B are large, then still FDE ≈ SWF, but a large fraction of strong winds are not accompanied by dust emission events, implying a large difference between T25 and T75. This could be caused by varying threshold behaviour due to changes in soil moisture or vegetation, for example. If B > C, then SWF > FDE and therefore a relatively large fraction of strong winds occur without dust. This

implies a rather abrupt start of emissions, and a larger difference between T50 and T75. If B < C, then SWF < FDE and therefore a relatively large fraction of weak winds create dust events, most likely accompanied by a larger difference between T25 and T50. Out of 18 387 observations of high winds with no emission from the 70 stations, 434 events (2.3 %) experienced a documented rainfall event in the previous 24 h. This provides evidence that some high-wind events do not produce dust due to high soil moisture. However, as the majority of rainfall values are blank in the SYNOP records, and we cannot ascertain if this is because there was no rainfall or no reading, we are cautious of using SYNOP precipitation to investigate this any further.

The SWF concept is used in the second method to determine an emission threshold. Here, SWF is first calculated for a range of wind-speed thresholds. The value that gives the smallest total squared difference between the seasonal mean diurnal cycles of FDE and SWF is then selected. A seasonal approach is preferred here in order to give stable PDFs. This method will be referred to as "least squares" (LS, hereafter). We expect it to give results of the same order as T50 and use it to test the robustness of the threshold identification approach. A comparison between the threshold values of T25, T50, T75 and LS gives more insight into the relationship between winds and emission than a single value and highlights the fact that emission occurs over a range of wind-speed values (Helgren and Prospero, 1987).

2.2.2 Dust-emitting power of winds: dust uplift potential

FDE provides occurrence frequency of emission, but not its intensity or quantity. To investigate the dust emitting power of the wind, we use the diagnostic parameter dust uplift potential (DUP; Marsham et al., 2011), based on the emission parameterisation of (Marticorena and Bergametti, 1995):

$$\mathrm{DUP} = U^3(1 + U_t/U)(1 - U_t^2/U^2) \quad (1)$$

for $U > U_t$, where U is the measured wind speed and U_t is a threshold wind speed for dust emission. DUP is zero when $U < U_t$. This diagnostic takes into consideration the highly non-linear impact of changes in winds on dust emission. DUP is very closely related to the power of the wind: if the land surface did not vary and the underlying emission parameterisation was accurate, dust emission would depend only on DUP. For DUP calculations, we use the seasonally varying T50 for U_t at each SYNOP station. The dust-emitting power per strong wind event is given by DUP mean (all DUP values, including 0 values)/fraction of strong wind events (SWF × 100) and is referred to as "DUP Intensity".

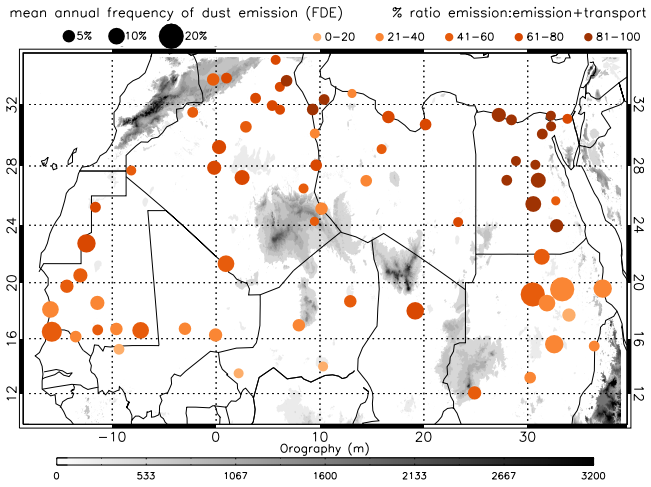

Figure 4. Annual emission climatology. Spatial distribution of mean annual FDE (dot size) and % ratio of emission to all dust events (including transported events) (dot colour) at 70 stations in northern Africa for the time period 1984–2012.

3 Results and discussion

3.1 Single-station climatologies

3.1.1 Annual frequencies of dust emission and transported dust

Figure 4 shows annual mean FDE for all stations for the entire investigation period 1984–2012. Despite a lot of variation between stations there are some general patterns in the geographical distribution. All 11 stations with FDE > 10 % are located between 15 and 23° N (large circles, Fig. 4). Situated close to an important dust source, the Bodélé Depression, Faya in Chad has a mean FDE of 12 %. Spatial variation is high in Egypt, particularly between the two stations of Kharga (10 %) and Luxor (1 %), which are within 230 km of each other. This could be due to local environmental factors, as Kharga is a desert oasis and Luxor is situated on the Nile. FDE values of 5 to 10 % are quite common in the northern Sahel and present at the central Algerian stations of Timimoun, Adrar and In Salah. Values < 5 % are frequent north of 24° N in the central and northern Sahara and in the southern Sahel. This pattern indicates that, although dust sources are found across the entire region, dust emission is generally more frequent in the semi-arid transition zone between the Sahel and Sahara (∼ 15–23° N). This is in agreement with the identification of a "Sahel dust zone" by Klose et al. (2010), though their study included transported events.

To explore the relative contribution of emission to all dust events at a given station, the ratio of emission to emission plus transport (BDF + DSF)/(BDF + DSF + TDF) (for definitions see Sect. 2.2.1) is displayed in Fig. 4 by the shading of circles, where light colours indicate more transport and dark colours more emission. Emission generally dominates

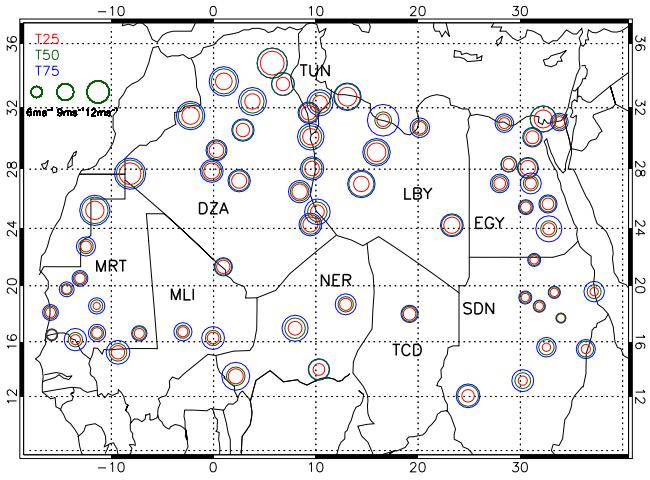

Figure 5. Geographical distribution of emission thresholds. Shown are annual values of T25, T50 and T75 (for definitions, see Sect. 2.2.1) in red, green and blue, respectively. Country codes, as defined by ISO: DZA = Algeria, TUN = Tunisia, MRT = Mauritania, MLI = Mali, NER = Niger, LBY = Libya, EGY = Egypt, TCD = Chad and SDN = Sudan.

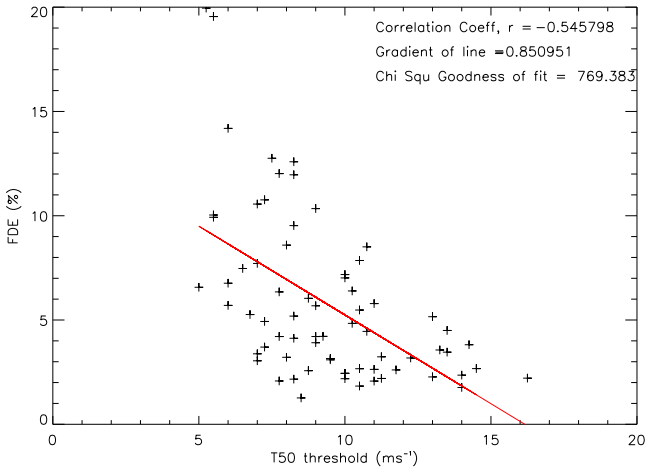

Figure 6. Scatter of annual mean frequency of dust events (FDE) against annual mean T50 (for definition, see Sect. 2.2.1) for each of the 70 individual stations for the period 1984–2012. Correlation coefficient, gradient of best-fit line and goodness of fit test are given in the top right corner.

the dust records north of $\sim 22°$ N. The largest values of > 90 % are found at many stations in Egypt. The Algerian and Tunisian stations of El Oued, Remada and El Borma (see Fig. 1 for locations) display a local maximum with values > 80 %. This area has been identified as a major dust source due to the dried lakes associated with Chott Jerid and Chott Melrhir (Prospero, 2002; Schepanski et al., 2012). Generally values > 50 % are found in Libya, Tunisia and Algeria, while for the majority of Sahelian stations values are < 50 %. Located close to active source regions, the stations of Bordj Mokhtar and Faya have transport ratios of 55 and 68 % respectively, which are among the highest of any stations south of 22° N. Transport events generally dominate Sahelian stations south of 20° N. Despite frequent transport reports, these stations also have FDE mean values comparable to those in the north, and sometimes higher, making the Sahel a dust hotspot (Klose et al., 2010). The dustiest subregion in northern Africa is Sudan with an FDE of more than 10 % at several stations and in addition to this, a high frequency of transport events. Overall, this analysis demonstrates that emission events contribute significantly to the frequency of all reported dust events, which includes transported dust, in this region.

3.1.2 Annual mean dust-emission thresholds

Spatial variations in annual mean dust emission thresholds are displayed in red, green and blue, representing T25, T50 and T75, in Fig. 5. Thresholds are generally higher north of 22° N, with T50 between 10 and 15 m s^{-1} at many stations in Algeria, Tunisia, central Libya and Niger. Moderate T50 values of 7–10 m s^{-1} are found in Egypt, southern Sudan and in parts of the west Sahelian countries of Mali and Mauritania. The lowest thresholds are found between 16° N and 20° N in the northern Sahel, in the west over Mauritania and particularly in central/northern Sudan, where T50 values of 5 m s^{-1} and 6 m s^{-1} are present at five adjacent stations. Differences between T25, T50 and T75 tend to be largest in the Sahel, consistent with possible influences from seasonal precipitation and vegetation there. Larger differences are also found for some stations along the Mediterranean coast, where occasional cool season rains may have a similar effect. There is no clear pattern in the relationship between T25, T50 and T75. For many stations, the three values are quite equally spaced. At some stations however, particularly in the Sahel, there is a much larger difference between T75 and T50 than between T25 and T50. This result suggests that these areas are occasionally characterised by soil states that do not allow dust emission, even for rather high winds. This could occur in summer when soils are wetter and more vegetated.

It is interesting to question the extent to which these spatial differences in thresholds affect dust emission or whether meteorological factors dominate. Figure 6 shows a scatter plot of annual mean FDE and T50 for all 70 stations plotted in Fig. 5. The anti-correlation of -0.54 shows that stations with low thresholds tend to have more frequent dust events, but the explained variance is only 30 %. The two prominent outliers are Dongola and Abu Hamed in Sudan, which have both very low thresholds and extremely high mean FDEs of almost 20 %. These high FDE values could be due to local environmental factors such as an easily erodible local source, or local orographic circulations which allow winds to exceed the threshold regularly.

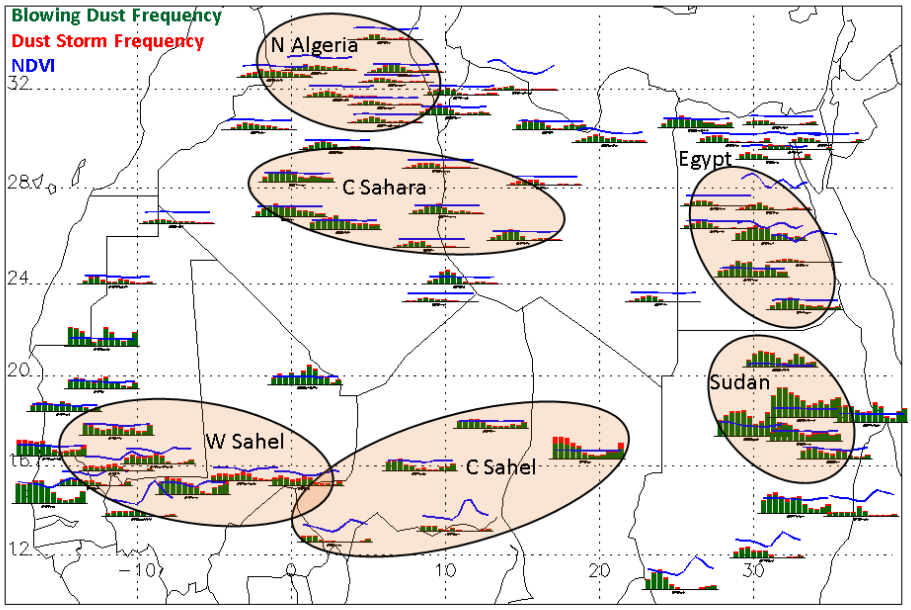

Figure 7. Mean seasonal cycle. Monthly mean FDE, split into BDF (green bars) and DSF (red bars) (for definitions, see Sect. 2.1.1), as well as monthly mean NDVI (blue lines) calculated for a 24 km × 24 km box centred on each station. The *x* axis runs from January to December. The *y* axis scale is 0–40 % for FDE and 0–5000 for NDVI. Areas of grouped stations, discussed in Sect. 3.2.1, are shown with shaded black ellipses and labels.

3.1.3 Seasonal cycles in frequency of dust emission and vegetation

Figure 7 shows station mean monthly values of FDE split into the contribution from BDF (green) and DSF (red). Each individual station plot can be found in Fig. S4 in the Supplement. Not surprisingly BDF dominates at all stations. DSF are quite rare, but relatively more common in the Sahel, particularly between 15 to 20° N. At many stations across Algeria, Tunisia, Libya, Egypt and Sudan FDE is highest in spring. The remaining stations, mostly situated in the central and western Sahel, have variable seasonal cycles, though most display reduced FDE in autumn. At the southernmost stations FDE is practically zero in late summer/early autumn when rainfall and vegetation cover are high. FDE peaks in summer at the central Saharan station Bordj Mokhtar, which could be related to the SHL and the arrival of convective cold pools from the northern Sahel during the peak of the summer monsoon as discussed in Marsham et al. (2013). Faya, the only station in Chad, shows high values of both FDE and DSF during the winter half year (Washington and Todd, 2005), when the harmattan is strongest, while monsoon-related summer dust storms are much rarer here.

Some of the seasonality evident from Fig. 7 is consistent with the seasonal cycle of vegetation cover. The most southerly stations, including Nioro Du Sahel, Niamey, Gouré, Nyala and El Obeid, show a marked increase in NDVI (blues lines in Fig. 7) in autumn following the summer rainfall maximum (Fensholt et al., 2012). These signals get weaker towards the northern Sahel and are absent in central Mauritania and at Bordj Mokhtar. In Egypt, the three stations situated on the banks of the Nile (Minya, Asyut and Luxor) contrast with desert oasis stations of Baharia, Farafra and Kharga, which have no seasonal cycle in vegetation. As the Nile river flow in Egypt is controlled by the upstream Aswan Dam, and this region experiences little rainfall, it is possible that the seasonal cycle is driven by agriculture and anthropogenic activities. There are some subtle changes in seasonal vegetation at northern Algerian stations, but overall in Algeria and Libya it is unlikely that vegetation has a major influence on seasonal dust cycles.

3.2 Climatologies from grouped stations

3.2.1 Rationale for grouping of stations

As discussed in the Introduction, there are numerous dust emitting mechanisms over northern Africa, creating distinct seasonal and diurnal cycles in different regions, while individual stations may also be influenced by very local factors such as topography or nearby obstacles (trees, buildings etc.). For further discussion of the climatology, six geographical groups of stations are defined: Northern Algeria (N Algeria hereafter), Central Sahara (C Sahara), Western Sahel (W Sahel), Central Sahel (C Sahel), Egypt and Sudan (see ellipses in Fig. 7). This was done subjectively by looking for similar characteristics in the seasonal and diurnal dust cycles as well as using literature and wind-direction climatologies to identify similar seasonal wind regimes. The reasoning behind

station selection in each group is discussed further below. Grouped values are calculated by taking a mean of a given variable (T25, T50, T75, LS, FDE, DBF, DSF, SWF, DUP mean), which has before been calculated separately for each station in the group. DUP Intensity is calculated after DUP and SWF have been group averaged first. Therefore each station is equally weighted within the group, but this comes with the caveat that stations with gaps and biases in their record are weighted equally to stations with more complete records.

N Algeria experiences a Mediterranean climate with wet winters, associated with Atlantic cyclones and Mediterranean depressions, and hot, dry summers (Warner, 2004). Saharan, or *Sharav* as they are known in NW Africa, cyclones are a key feature here in spring (Hannachi et al., 2011) and play a role in dust source activation (Schepanski, 2009; Fiedler et al., 2013b). Analysis of the wind direction (not shown) suggests that the background flow, hence large-scale influence, are similar at the stations of Biskra, El Oued, Touggourt, Ghardaia, Elbayadh, Hassi Messaoud, Ouargla and Mecheria which make up the N Algeria group. Quality flags of 1 apply to all eight stations due to unbiased and unbroken time series of data (Fig. 1). Six of the eight stations are situated in the low-lying area to the southeast of the Atlas Mountains, while Mecheria and Elbayadh are located in the foothills and have elevations of 1149 m and 1347 m, respectively.

The C Sahara group is situated further south, between 27–30° N, and 1° W–14° E. The stations of Timimoun, Adrar, In Salah, In Amenas, Ghadames and Sebha experience a different meteorological regime to that of N Algerian stations. Rainfall is scarce and winds, which are generally higher, have an easterly or northeasterly direction. Similar to N Algeria, all stations have a quality flag of 1 (Fig. 1) and show a peak in FDE in spring (Fig. 7). In Egypt, we focus on the seven inland stations of Baharia, Farafra, Kharga, Minya, Asyut, Luxor and Aswan within the region 23–28° N, 27–33° E which are characterised by a similar N–NW wind regime. Only Farafra has quality issues, with 1B flag indicating a period > 5 years with reduced observations (Fig. 1). Despite some seasonal variation in the vegetation cycle at stations on the banks of the Nile (Minya, Asyut and Luxor, see Fig. 7), the overall seasonal cycle of dust is similar with a spring peak in FDE, most likely caused by the seasonality of meteorological factors.

Two groups of stations in the Sahel are considered. The W Sahel group is comprised of the inland stations of Kiffa, Aioun El Atrouss, Nioro Du Sahel, Kaedi, Nema, Tombouctou, Gao and Tidjika, and encompasses the region 13–19° N, 13° W–0° E. The C Sahel stations include Bilma, Niamey, Gouré and Agadez in Niger and Faya in Chad. The main difference between the two groups is that the summer monsoon and its interactions with the SHL drive summer emissions in W Sahel, but have less influence over the C Sahel stations, which are united by the domination of the winter harmattan winds as a driver of the frequency of dust emission (Fig. 7). As is common with nearly all Mauritanian stations, five of the eight stations in the W Sahel group have a daytime bias and four have gaps of < 5 years as indicated with flags of 2 and A respectively (Fig. 1). The quality of C Sahel stations is mixed, with healthy stations of Niamey and Gouré achieving quality flags of 1, in contrast to Faya with a 2B flag (Fig. 1).

The Sudan group consists of Wadi Halfa, Abu Hamed, Dongola, Karima and Atbara and lies within the coordinates 17–22° N, 30–34° E. This excludes the southern stations, where the influence of the monsoon is felt in summer. Only Atbara receives small amounts of summer rains. From Karima up to Wadi Halfa, the stations remain in a consistently northerly flow and experience almost no rainfall. B quality flags apply to these stations to indicate gaps in the record > 5 years, which coincide with periods of civil unrest (Fig. 1).

3.2.2 Seasonal cycle in dust-emission thresholds

To summarise and complement the discussion based on Fig. 5 in Sect. 3.1.2, seasonal values of T25, T50, T75 and LS dust emission thresholds are presented here (Fig. 8), which are first calculated for each station and then averaged over the group. The LS values are typically within $1\,\mathrm{m\,s^{-1}}$ from T50, but deviations of up to $2.5\,\mathrm{m\,s^{-1}}$ also occur for some groups in some seasons. Consistent with Fig. 5, Fig. 8 shows that the highest thresholds are observed at the N Algeria stations with an annual mean of $11.5\,\mathrm{m\,s^{-1}}$ followed by the C Sahara group. The lowest thresholds are observed in Sudan with a mean of $5.7\,\mathrm{m\,s^{-1}}$. The maximum seasonal threshold of $12.5\,\mathrm{m\,s^{-1}}$ occurs in the wet N Algerian winter, while Sudan thresholds fall to a minimum of $5.5\,\mathrm{m\,s^{-1}}$ in spring.

Seasonal variability is highest in the summer monsoon-influenced Sahel, particularly the C Sahel where thresholds are a mean of $2.8\,\mathrm{m\,s^{-1}}$ higher in summer than in winter. In contrast to this Sudan thresholds vary by only $0.5\,\mathrm{m\,s^{-1}}$. The seasonal transition from low thresholds to high thresholds takes place in summer in W Sahel and in spring in the C Sahel, where two of the southernmost stations are located. In both regions T75 increases before T50 and T25. We hypothesise that this is due to infrequent early-season precipitation events, which moisten soils so that no emission can take place. Just a few of these events could create the increase in D75, while for the majority of the time it is still dry enough to allow for dust emission such that T25 and T50 do not rise similarly.

Standard deviations in thresholds between stations within each group (indicated by error bars in Fig. 8) are largest in summer in the C Sahara and C Sahel, in winter in N Algeria and in autumn in the W Sahel and Egypt. Interestingly these increases in spatial variability within a region are usually accompanied by an increase of the threshold itself. This may indicate that the changes in soil moisture and vegetation that cause the threshold to rise are inhomogeneous across the region. However, higher thresholds typically also coincide

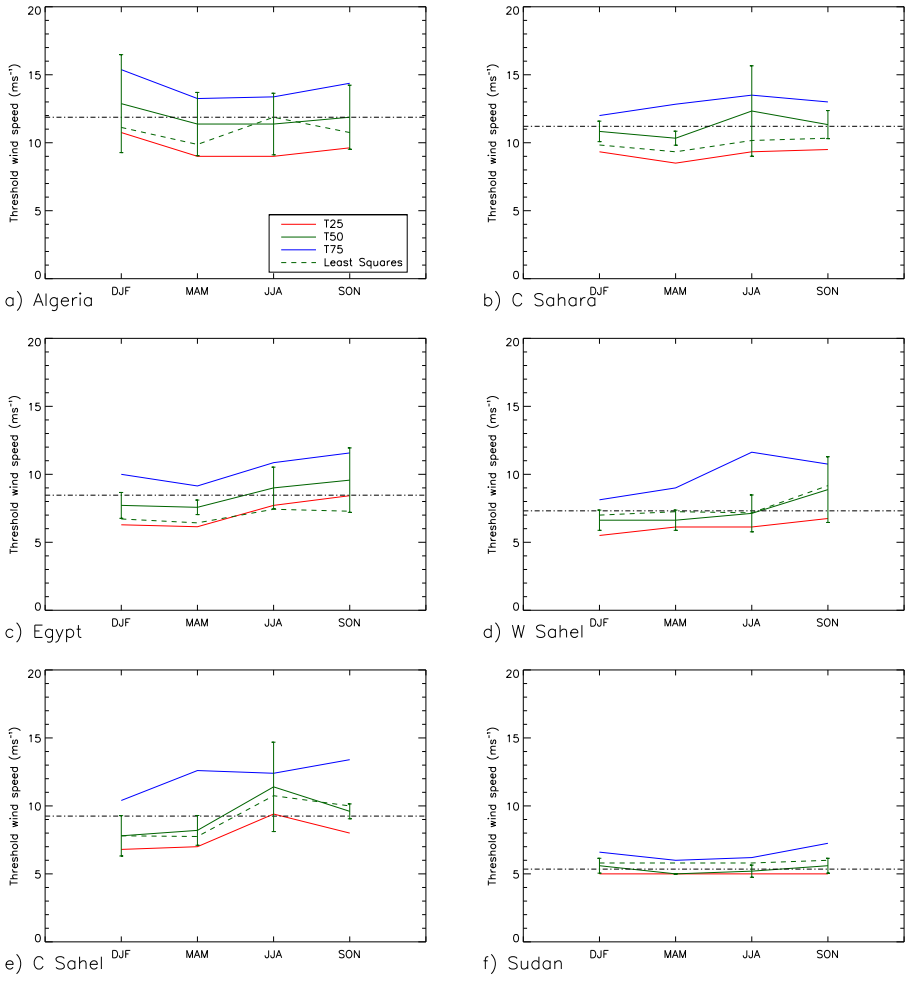

Figure 8. Seasonal threshold values averaged over six station groups (see Sect. 3.2.1 for definition): **(a)** N Algeria, **(b)** C Sahara, **(c)** Egypt, **(d)** W Sahel, **(e)** C Sahel and **(f)** Sudan according to the legend in the top left panel (for definition of thresholds, see Sect. 2.2.1). The dashed black lines indicate the annual mean T50. Seasons are December, January, February (DJF), March, April, May (MAM), June, July, August (JJA) and September, October, November (SON).

with fewer dust observations, which reduces confidence in the threshold estimates.

3.2.3 Seasonal cycle in dust emission

Figure 9 shows the seasonal evolutions of BDF, DSF and FDE (bars) together with those of SWF, DUP and DUP Intensity (lines) for the six groups. The latter three are based on seasonal, rather than monthly, T50 values (season boundaries are indicated by thin vertical lines in Fig. 9). This slight inconsistency is undesirable, but necessary to obtain sufficient data to estimate stable thresholds. The influence of using seasonal, instead of annual mean, thresholds is rather insignificant and consistent with the relatively minor changes seen in Fig. 8. For example, monthly correlations between FDE and SWF vary on average by only 0.08 from when using either a seasonally varying, or a fixed annual mean, T50 threshold.

Spring is the dominant season in the N Algeria group as expected from Fig. 7, with a maximum FDE of 7 % in April. DSF is very low in this region throughout the year with largest values also in April. The annual cycle of SWF follows that of FDE closely with a correlation of 0.99, but with values consistently 1–2 % lower. As discussed in Sect. 2.2.1, this implies a relatively large area C (winds below T50 which do produce emission) in Fig. 2 and is consistent with the slightly larger difference between T50 and T25 than that between T50 and T75 in Fig. 8a. As the region with the highest threshold of all groups, T25 is already well above typical emission thresholds found in the literature (Helgren and Prospero, 1987; Chomette et al., 1999), creating this rather broad range of wind speeds which can and cannot produce dust. The annual cycle of DUP agrees with FDE on the overall peak in spring. The ratio of DUP to SWF ("DUP Intensity") indicates a relatively low mean intensity from February

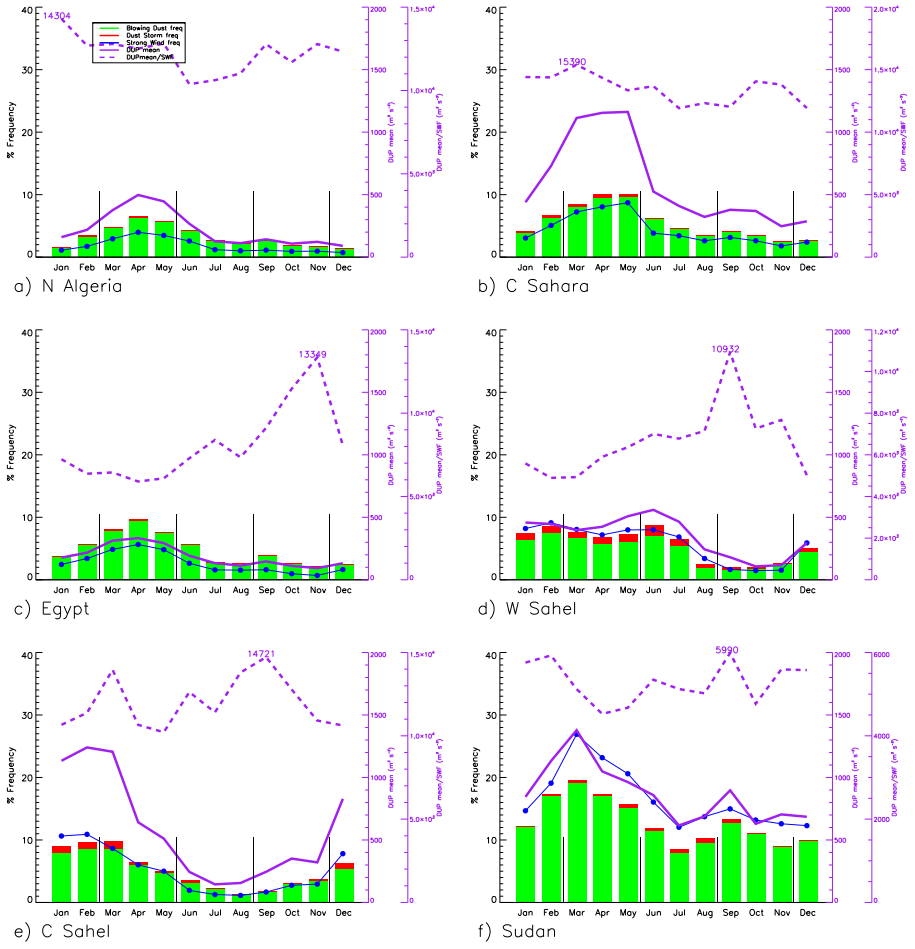

Figure 9. Mean seasonal cycle for the six station groups (see Sect. 3.2.1 for definitions): **(a)** N Algeria, **(b)** C Sahara, **(c)** Egypt, **(d)** W Sahel, **(e)** C Sahel and **(f)** Sudan. Monthly frequency of FDE, split into BDF (green bars) and DSF (red bars), as well as SWF (blue line), DUP mean (solid purple) and DUP Intensity (DUP mean/SWF, dashed purple, maximum values given), all computed using the seasonally varying T50 (for definitions of parameters, see Sect. 2.2.1). Thin vertical black lines indicate seasonal boundaries where thresholds change. Note the different vertical axes for DUP intensity.

to July and much higher values from September to January. This suggests that less frequent dust events during the cool season are more intense when they occur. Mediterranean cyclones could be the meteorological mechanism creating high-intensity events in the cool season. As shown by Fig. 8a, winter is also the time when thresholds are slightly increased, requiring a more extreme meteorological event to generate dust.

Several of these features are broadly reproduced in the C Sahara (Fig. 9b), but values of both FDE and DUP are significantly higher than in N Algeria (note identical FDE and DUP scales in all panels of Fig. 9). Here, FDE peaks at 10 % in April with a secondary autumn maximum in both DUP and FDE which is less significant than the spring maximum. DUP Intensity is less seasonally variable than in N Algeria with typical values around $14\,000\,m^3\,s^{-3}$, which is slightly lower than in N Algeria (note the variable DUP Intensity scales between panels in Fig. 9). Egypt (Fig. 9c) also agrees with the former two regions with respect to the spring maximum and secondary maximum in autumn FDE. The annual FDE peak is 10 % in April and the annual mean is ~ 2 % higher than N Algeria. SWF is considerably lower here than FDE but shows a similar annual cycle. Less frequent strong winds could, to some extent, explain the lower DUP mean values. The clearest difference is the clear peak in DUP Intensity in November, though overall DUP Intensity is lower than N Algeria and C Sahara. High DUP Intensity in autumn could be due to occasional storms from the Mediterranean affecting northeastern Africa, during a time when thresholds are slightly increased (Fig. 8c).

Behaviour is fundamentally different over the two Sahelian regions (Fig. 9d and e). A similar effect on dust concentration was observed by Marticorena et al. (2010) for two stations located within the C and W Sahel regions. The C Sahel,

which contains more southern stations, displays a longer low dust season. W Sahel is located closer to the centre of the SHL in summer, which may contribute to dust emissions into June and even July. In both regions the agreement in magnitude between FDE and SWF is better than for the three northern regions, indicating a better balance between low winds with dust and high winds without dust. Annual mean DSF is higher than in the three northern regions, possibly pointing to more productive dust sources. DUP mean and SWF correlate well with FDE (0.94 and 0.98, respectively) in W Sahel with absolute values similar to N Algeria. DUP Intensity is lowest in winter, despite February being the month of highest FDE. This could be due to the lack of haboobs in this season which have a significant contribution to DUP the rest of the year. The annual cycle in FDE is very different in the C Sahel. Both DUP and SWF have correlations of 0.97 with FDE, but here the winter is the only main dust season, driven by strong NE harmattan winds and frequent LLJ breakdown in this season (Washington et al., 2006; Schepanski et al., 2009). The southern stations in this region have a clear vegetation increase in autumn (Fig. 7) which could also decrease FDE levels and contribute to higher dust emission thresholds (Fig. 8e), though this may not necessarily be representative of the more northern and arid stations of Bilma and Faya (Fig. 1). Extremely intense, local emissions were found to be important to dust concentrations in Marticorena et al. (2010) in the Sahel summer months, associated with the passage of mesoscale convective systems (MCSs). However, with their short durations of less than 1 h at the observation stations, MCSs may not be properly represented by the 3-hourly SYNOP data used here.

It is interesting to compare the C and W Sahel regions with that at Bordj Mokhtar, immediately to the north of the Sahel (Fig. 10). High year-round dust emission reaches a maximum of 18 % in July, followed by August and June and all three months have high DSF. This summer maximum is also identified in TOMS AI measurements (Engelstaedter and Washington, 2007). This station is too far north to get enough monsoonal precipitation to suppress source strength. However, it is likely that cold pools from Sahelian squall lines could reach Bordj Mokhtar during the summer to cause the observed peak. This leads to high DUP values in June, July and August, likely underestimated due to the fact that only daytime cold pools are detected (no data from 21:00–03:00 UTC) which will have weakened by the time they reach the station, if formed the previous night.

Northern Sudan (Fig. 9f) stands out as having the highest FDE year-round (annual mean of 13 %), though DUP values are not comparably increased, suggesting frequent lower-energy events. DSF is a little higher than in the three northern regions here, particularly during June–September, but not as high as in the W and C Sahel. The most active month is March with an FDE of 20 %, while September shows a secondary peak similar to that in the three northern groups (Fig. 9a–c). DUP Intensity is the lowest of the six regions but peaks during the second maximum in September. SWF is consistently higher than FDE (annual mean of 17 %), but with a similar annual cycle resulting in a correlation of 0.95. This may well be a reflection of the very low threshold in this region (Fig. 8f), below which dust emission will be very rare.

3.2.4 Diurnal cycle and meteorological mechanisms

The 3-hourly resolution of SYNOP reports also allows the investigation of seasonal mean diurnal cycles of FDE, DUP and DUP Intensity (as defined in Figs. 9 and 10) for each group (Figs. 11 and 12). For N Algeria (left column of Fig. 11), there are stark contrasts between day and night during all seasons. Maximum FDE is at 15:00 UTC (16:00 local time, LT) in all seasons but summer, when values are slightly higher at 12:00 UTC and emission extends longer into the night. The minimum is at 06:00 UTC year-round. The diurnal cycle of DUP largely follows that of FDE with some minor shifts, such as a maximum at 12:00 UTC in winter and autumn. Consistent with previous discussions, FDE and DUP reach comparable magnitudes in winter, summer and autumn, but are higher in spring (note the different scales). DUP Intensity tends to oppose the FDE and DUP diurnal cycles, with peaks at night and smaller values during the day, though this is less pronounced in N Algeria spring (Fig. 11b). During winter and autumn, when nights are comparably long and column water vapour tends to be low, radiative cooling can create strong surface inversions that can only be broken by the strongest storms with wind speed well above the emission threshold, leading to fewer events with larger DUPs. This behaviour is still evident in summer and spring, but less pronounced. Overall, the diurnal cycle found for this region suggests that NLLJ breakdown in the morning could play a role, leading to rapid increases in FDE and DUP between 06:00 and 12:00 UTC. The continuation of high values into the afternoon, when the boundary layer typically is deepest, indicates additional momentum sources above that of the NLLJ. These are likely related to thermal wind contributions caused by baroclinic zones due to mountains (Stensrud, 1996), land–sea contrasts (Todd et al., 2013) or the presence of the subtropical jet. The growth of the boundary layer due to heating of the surface will also contribute by accessing these upper level thermal wind contributions around 12:00–15:00 UTC and mixing down more intense turbulence. In summer, the extension of FDE and DUP into the evening may be related to convective cold pools as discussed in Knippertz et al. (2007) for the Atlas Mountains and in Emmel et al. (2010) for Morocco.

The C Sahara regions (middle column in Fig. 11) also shows a marked day–night contrast, but with some remarkable deviations from N Algeria. The FDE maximum is at 09:00 UTC in all seasons but winter (where it is 12:00 UTC), suggesting a relatively more important role of the morning breakdown of NLLJs. This is most likely related to a larger distance from baroclinic zones, which reduces the likelihood

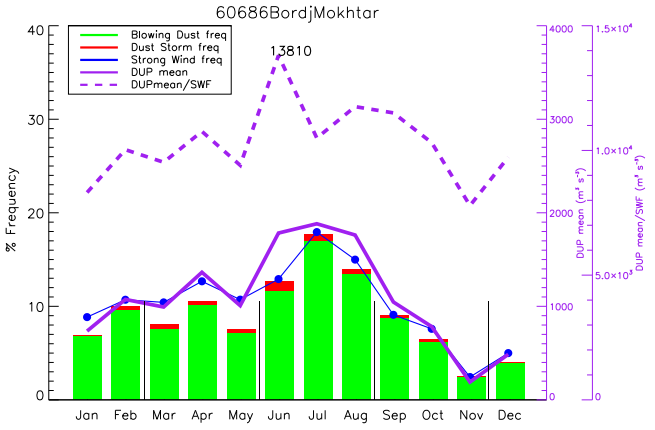

Figure 10. As Fig. 9 but for Bordj Mokhtar (WMO number 60686).

of afternoon LLJ breakdown as the boundary layer grows. An additional factor could be that LT is slightly later for the Libyan stations in this region, possibly resulting in some later emissions being included at an earlier SYNOP hour. Consistent with previous figures, FDE and DUP are highest in spring, followed by summer and winter, then lowest in autumn. DUP Intensity drops during the day in summer and autumn, but actually increases in winter and spring daytime following a dip before sunrise. Diurnal DUP Intensity varies less in winter and spring and dips before sunrise in contrast to summer and autumn where DUP Intensity is high at night. In summer, when nights are relatively short and stability is weaker, early breakdowns of NLLJ could play a role as well as ageing cold pools from afternoon convection over the Hoggar Mountains.

In Egypt (right column in Fig. 11) diurnal cycles in FDE and DUP are stable throughout the year with minimum at 03:00 UTC (05:00 LT) and maximum at 12:00 UTC (14:00 LT), suggesting some influence of NLLJ breakdown, deep boundary layer mixing during the afternoon and perhaps the general presence of daytime dry convection. DUP Intensity is consistent all year, with a peak at 03:00 UTC and minimum at 15:00 UTC. This is related to the diurnal cycle of stability as discussed before.

The analysis of the diurnal cycles in W and C Sahel is complicated by fewer night-time observations compared with daytime (2 in quality flags, Fig. 1). This introduces larger random error in night-time values in these locations. This is unfortunate, as convective cold pools are expected to affect these regions during the evening and night. Both groups of stations show a clear daytime peak in FDE all year. In the W Sahel (left column of Fig. 12) this occurs at 12:00 UTC, in the C Sahel (middle column of Fig. 12) at 09:00 UTC (10:00 LT), suggesting a strong influence of the NLLJ in all seasons. The DUP Intensity cycle is consistent with the other regions; low during the day and high at night. Any sharp increases in DUP and DUP Intensity at night, such as 21:00 UTC (Fig. 12f and g) and 18:00 (Fig. 12h), are possibly artefacts of the low number of observations at this reporting time which allow a small number of individual events, possibly only reported because they are exceptional, to dominate the statistics.

In Sudan (right column of Fig. 12) FDE shows again maxima at 09:00–12:00 UTC (14:00 LT) in winter and spring, and only 09:00 UTC (11:00 LT) in summer and autumn. FDE remains relatively high during the night, too, with values never dropping below 5 %. When compared to the diurnal cycle of N Algeria (Fig. 11) where emission never exceeds 5 % in winter, summer or autumn, this highlights the strong permanent presence of dust emission in Sudan. The high values at night in Sudan could be due to orographic flow in the Nile valley, indicated by consistent dips in emission just before and after sunrise, or occasional haboob storms in summer. DUP and DUP Intensity show relatively flat diurnal cycles, with lower intensities during the second half of the day, which suggests weaker events or an overestimation of emission by the observer due to the already high dust levels in the atmosphere.

4 Conclusions

This is the first detailed analysis of dust emission from long-term surface SYNOP observations over the Saharan and Sahel region. Data quality is a major issue in this area and we attempt to balance quality of the data set with spatial coverage by including imperfect station records and making their limitations clear. Initial criteria were used to eliminate extremely biased and patchy stations or those that simply did not have enough dust reports to make meaningful statistics from, which left 70 stations to work with. Quality flags assigned to these stations gave indications as to the results that should be approached with caution, such as the diurnal cycle in the Sahel where a daytime bias is present. Frequency of dust emission (FDE) is compiled from present weather reports of 7–9, 30–35 and 98 divided by the total number of reports. These statistics are further split into dust storm frequency (DSF) which includes only reports of 9, 30–35 and 98 and blowing dust frequency (BDF) with associated reports of 7 or 8. Dust uplift potential (DUP, Marsham et al., 2011) is used to investigate the dust emitting power of the wind. Strong wind frequency (SWF) is calculated in the same way as FDE but using 10 m surface winds over a threshold instead of dust emission reports. Reports over 55 kn are excluded due to low confidence in their accuracy. DUP Intensity is DUP mean per SWF and gives an indication of the type of dust events which might be occurring. The regional differences in the seasonal and diurnal cycles of dust emission were presented and discussed by subjectively separating stations into six groups with similar meteorological regimes.

Thresholds were determined objectively in two ways. First, by comparing the PDFs of dust emission and windspeed observations to give the 25, 50 and 75 % probabilities

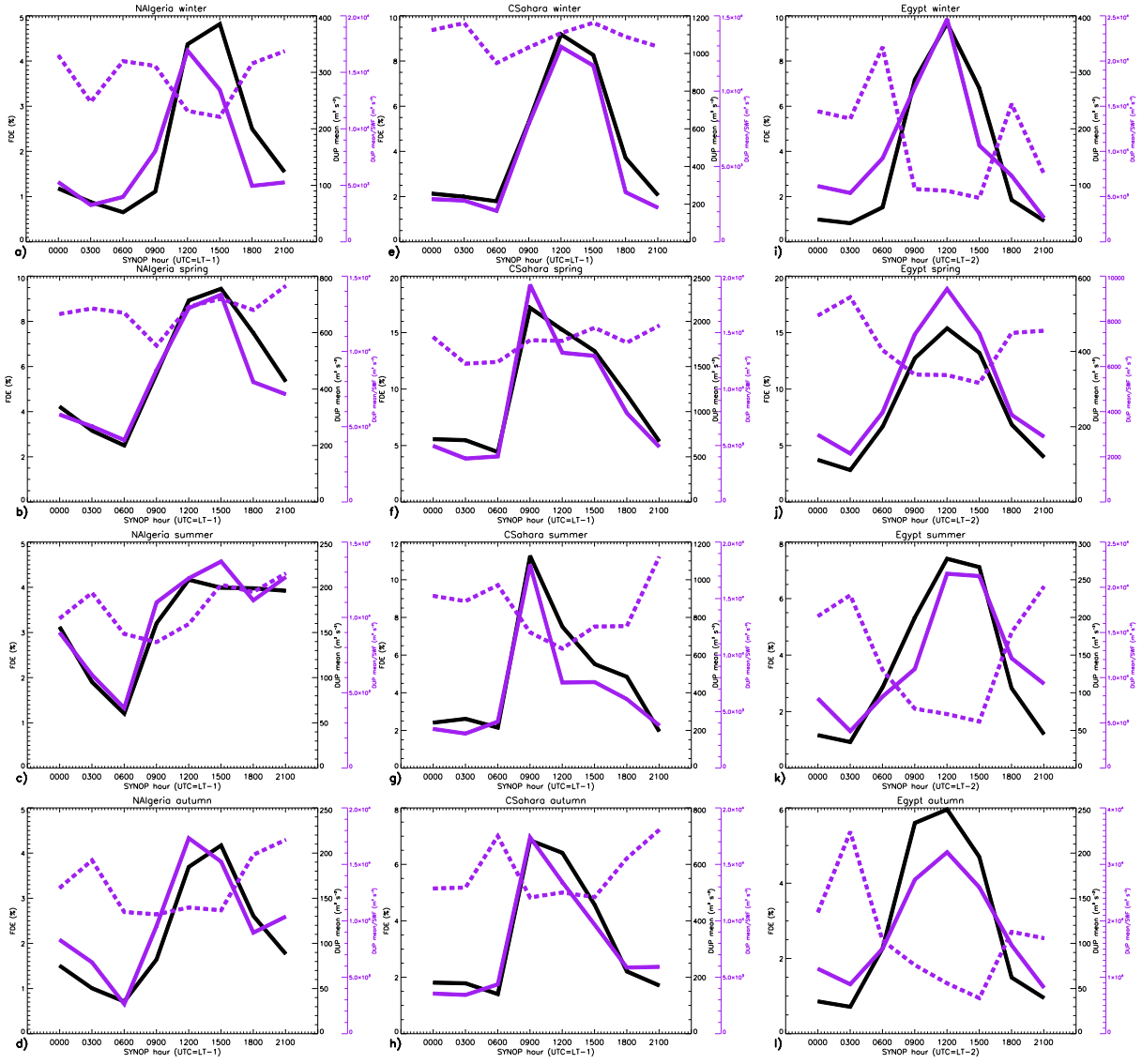

Figure 11. Diurnal cycles of FDE (solid black), DUP mean (solid purple) and DUP Intensity (dashed purple) for N Algeria (column 1), C Sahara (column 2) and Egypt (column 3) for DJF (row 1), MAM (row 2), JJA (row 3) and SON (row 4) (see Sect. 3.2.1 for definition of regions). For definitions of parameters, see Sect. 2.1.1.

of dust emission and second, by calculating the least squares difference in the diurnal cycle of the frequency of both dust emission (FDE) and strong winds (SWF). Annual mean grouped thresholds range from 5.7 m s^{-1} in Sudan to 11.5 m s^{-1} in N Algeria. In general, thresholds are higher in the hyper-arid Sahara north of 22° N. Seasonal variations in thresholds are largest in the Sahel and smallest in Sudan. In arid Sudan (this work focuses on the northern stations of Sudan) there is significantly less rainfall than in the Sahel. Hence, there will be less seasonal variation in soil characteristics leading to less-variable thresholds in Sudan. There is also evidence of soil moisture varying in time when T75 increases before T25 in the Sahel transition from high- to low-emission seasons.

Spatially, annual mean observed emission is highest between 16 and 24° N. Emission events are more frequent than transported events north of 24° N, while south of this, although FDE is high, the frequency of transported events is even higher. This highlights the overall more frequent presence of dust in the atmosphere south of 24° N (Klose et al., 2010). Outside the Sahel, FDE and DUP peak in spring, related to strong pressure gradients in this season. The Sahel does have high emission in spring but the seasonal cycle is more complex with the influences of both the Saharan Heat Low and monsoon-related haboobs, which create

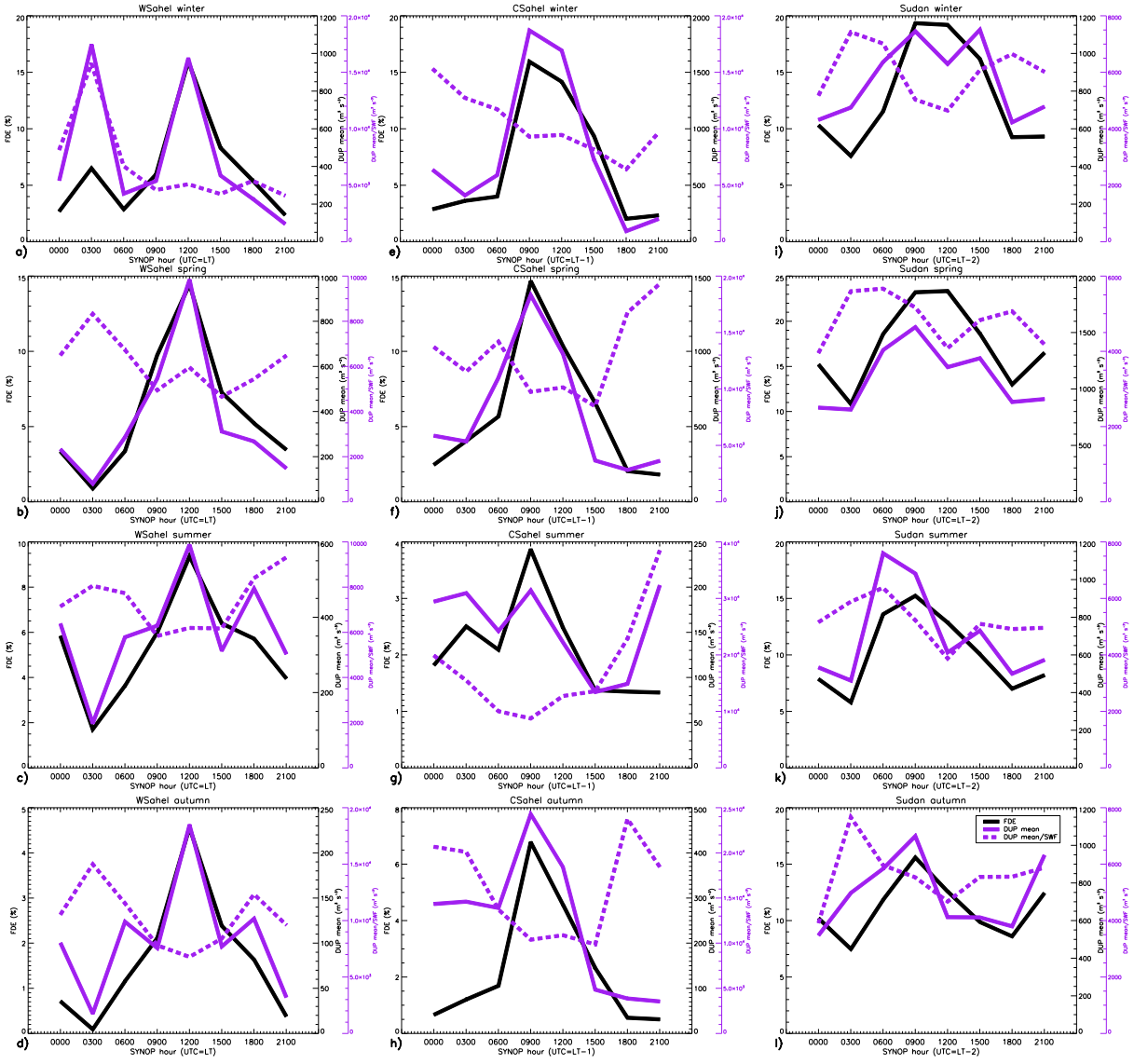

Figure 12. Diurnal cycles of FDE (solid black), DUP mean (solid purple) and DUP Intensity (dashed purple) for W Sahel (column 1), C Sahel (column 2) and Sudan (column 3) for DJF (row 1), MAM (row 2), JJA (row 3) and SON (row 4) (see Sect. 3.2.1 for definition of regions). For definitions of parameters, see Sect. 2.1.1.

more summer emission in the W Sahel, but hardly affect the C Sahel. In the C Sahel a particularly strong harmattan flow, with embedded NLLJs, create strong emissions in winter and early spring. Bordj Mokhtar (southern Algeria), the only station between the Sahel and the central Sahara, has a strong summer peak in FDE and DUP. Despite an absence of night-time data, the presence of haboobs at this location in the Sahara is indicated by the jump in FDE, DUP and DUP Intensity in June.

Seasonal variation in emission frequency is mostly controlled by strong wind frequency, indicated by high correlations between FDE and SWF in all areas, which changes little when SWF is calculated with a seasonally variable or annually fixed threshold. However, the relationship between FDE and DUP is more complex, as more frequent events do not necessarily mean more emission. DUP is most closely related to FDE in the C Sahara, and so intensity (DUP per SWF) is relatively constant. This shows that here the strength of the winds that generate emission does not vary much seasonally. DUP and FDE are typically higher during the day, relative to night, when atmospheric stability increases and inhibits strong winds. As a consequence, any emission which does take place is likely to require a stronger wind in order to overcome this stability. High night-time DUP Intensity values support this conclusion.

Our results are consistent with currently understanding of vegetation growth in the Sahel and its role in decreasing emissions in late summer and autumn. We find high levels of summer emissions in the SHL region, despite the fact that the only station in this area, Bordj Mokhtar, may be missing up to 50 % of emission events (Marsham et al., 2013) through absent night-time observations. The NLLJ is observed in the diurnal cycle of Niger and Chad stations which is in line with past work close to the Bodélé Depression by Washington et al. (2006, 2009). Evidence here suggests that NLLJs, creating frequent morning emission, are the dominant mechanism in the central Sahara and central Sahel, while in other regions it is difficult to separate NLLJ breakdown from other factors, such as boundary layer growth eroding daytime LLJs. These daytime LLJs can be formed in response to complex terrain, mountains or land–sea air temperature contrasts.

The results of this climatology are a stepping stone towards improving our understanding of the overall mechanisms which influence the frequency of dust events and strong winds. By characterising the data set limitations and advantages we are in a better position to use it to evaluate other data sets such as reanalyses, output from dust models and satellite data, which come with their own caveats. Moving on from the work presented here we aim to combine these results with additional information from reanalysis data to further explore the relative contribution of different mechanisms to the dust cycle.

The Supplement related to this article is available online at doi:10.5194/acp-14-8579-2014-supplement.

Acknowledgements. This work is funded by the European Research Council as part of the "Desert Storms" project under grant 257543. We acknowledge support by Deutsche Forschungsgemeinschaft and the Open Access Publishing Fund of Karlsruhe Institute of Technology. NDVI is compiled from Advanced Very High Resolution Radiometer data and is available from the Global Inventory Modeling and Mapping Studies (GIMMS) database (www.landcover.org) for the time period 1984–2006.

Edited by: X. Querol

References

Ackerman, S. and Cox, S.: Surface Weather Observations Of Atmospheric Dust Over the Southwest Summer Monsoon Region, Meteorol. Atmos. Phys., 41, 19–34, doi:10.1007/BF01032587, 1989.

Allen, C. J. T., Washington, R., and Engelstaedter, S.: Dust emission and transport mechanisms in the central Sahara: Fennec ground-based observations from Bordj Badji Mokhtar, June 2011, J. Geophys. Res.-Atmos., 118, 6212–6232, doi:10.1002/jgrd.50534, 2013.

Bagnold, R.: The physics of blown sand and desert dunes, Dover Publications, Mineola, NY, USA, 85–95, 1941.

Bou Karam, D., Flamant, C., Knippertz, P., Reitebuch, O., Pelon, J., Chong, M., and Dabas, A.: Dust emissions over the Sahel associated with the West African monsoon intertropical discontinuity region: A representative case-study, Q. J. Roy. Meteor. Soc., 134, 621–634, 2008.

Bristow, C. S., Hudson-Edwards, K. A., and Chappell, A.: Fertilizing the Amazon and equatorial Atlantic with West African dust, Geophys. Res. Lett., 37, L14807, doi:10.1029/2010GL043486, 2010.

Chomette, O., Legrand, M., and Marticorena, B.: Determination of the wind speed threshold for the emission of desert dust using satellite remote sensing in the thermal infrared, J. Geophys. Res.-Atmos., 104, 31207–31215, 1999.

Cowie, S. M., Knippertz, P., and Marsham, J. H.: Are vegetation-related roughness changes the cause of the recent decrease in dust emission from the Sahel?, Geophys. Res. Lett., 40, 1868–1872, doi:10.1002/grl.50273, 2013.

Dufresne, J., Gautier, C., Ricchiazzi, P., and Fouquart, Y.: Longwave scattering effects of mineral aerosols, J. Atmos. Sci., 59, 1959–1966, doi:10.1175/1520-0469(2002)059<1959:LSEOMA>2.0.CO;2, 2002.

Emmel, C., Knippertz, P., and Schulz, O.: Climatology of convective density currents in the southern foothills of the Atlas Mountains, J. Geophys. Res.-Atmos., 115, D11115, doi:10.1029/2009JD012863, 2010.

Engelstaedter, S. and Washington, R.: Atmospheric controls on the annual cycle of North African dust, J. Geophys. Res.-Atmos., 112, D03103, doi:10.1029/2006JD007195, 2007.

Evan, A. T., Heidinger, A. K., and Knippertz, P.: Analysis of winter dust activity off the coast of West Africa using a new 24-year over-water advanced very high resolution radiometer satellite dust climatology, J. Geophys. Res.-Atmos., 111, D12210, doi:10.1029/2005JD006336, 2006.

Fensholt, R., Langanke, T., Rasmussen, K., Reenberg, A., Prince, S. D., Tucker, C., Scholes, R. J., Le, Q. B., Bondeau, A., Eastman, R., Epstein, H., Gaughan, A. E., Hellden, U., Mbow, C., Olsson, L., Paruelo, J., Schweitzer, C., Seaquist, J., and Wessels, K.: Greenness in semi-arid areas across the globe 1981-2007 - an Earth Observing Satellite based analysis of trends and drivers, Remote Sens. Environ., 121, 144–158, doi:10.1016/j.rse.2012.01.017, 2012.

Fiedler, S., Schepanski, K., Heinold, B., Knippertz, P., and Tegen, I.: Climatology of nocturnal low-level jets over North Africa and implications for modeling mineral dust emission, J. Geophys. Res.-Atmos., 118, 6100–6121, doi:10.1002/jgrd.50394, 2013a.

Fiedler, S., Schepanski, K., Knippertz, P., Heinold, B., and Tegen, I.: How important are cyclones for emitting mineral dust aerosol in North Africa?, Atmos. Chem. Phys. Discuss., 13, 32483–32528, doi:10.5194/acpd-13-32483-2013, 2013b.

Forster, P., Ramaswamy, V., Artaxo, P., Berntsen, T., Betts, R., Fahey, D. W., Haywood, J., Lean, J., Lowe, D. C., Myhre, G., Nganga, J., Prinn, R., Raga, G., Schulz, M., and Van Dorland, R.: Changes in Atmospheric Constituents and in Radiative Forcing. In: Climate Change 2007: The Physical Science Basis. Contribution of Working Group I to the Fourth Assessment Report of the Intergovernmental Panel on Climate Change, Tech. rep., 2007.

Gillette, D., Adams, J., Endo, A., Smith, P. H., D., and Kihl, R.: Threshold velocities for input of soil particles into the air by

desert soils, J. Geophys. Res.-Ocean. Atmos., 85, 5621–5630, doi:10.1029/JC085iC10p05621, 1980.

Ginoux, P., Prospero, J. M., Gill, T. E., Hsu, N. C., and Zhao, M.: Global scale attribution of anthropogenic and natural dust sources and their emission rates based on MODIS Deep Blue aerosol products, Rev. Geophys., 50, RG3005, doi:10.1029/2012RG000388, 2012.

Goudie, A. S. and Middleton, N. J.: Saharan dust storms: nature and consequences, Earth-Science Reviews, 56, 179–204, 2001.

Hannachi, A., Awad, A., and Ammar, K.: Climatology and classification of Spring Saharan cyclone tracks, Climate Dynamics, 37, 473–491, doi:10.1007/s00382-010-0941-9, 2011.

Heinold, B., Knippertz, P., Marsham, J. H., Fiedler, S., Dixon, N. S., Schepanski, K., Laurent, B., and Tegen, I.: The role of deep convection and nocturnal low-level jets for dust emission in summertime West Africa: Estimates from convection-permitting simulations, J. Geophys. Res.-Atmos., 118, 4385–4400, doi:10.1002/jgrd.50402, 2013.

Helgren, D. M. and Prospero, J. M.: Wind Velocities Associated With Dust Deflation Events in the Western Sahara, J. Clim. Appl. Meteorol., 26, 1147–1151, 1987.

Huber, S. and Fensholt, R.: Analysis of teleconnections between AVHRR-based sea surface temperature and vegetation productivity in the semi-arid Sahel, Remote Sens. Environ., 115, 3276–3285, doi:10.1016/j.rse.2011.07.011, 2011.

Huneeus, N., Schulz, M., Balkanski, Y., Griesfeller, J., Prospero, J., Kinne, S., Bauer, S., Boucher, O., Chin, M., Dentener, F., Diehl, T., Easter, R., Fillmore, D., Ghan, S., Ginoux, P., Grini, A., Horowitz, L., Koch, D., Krol, M. C., Landing, W., Liu, X., Mahowald, N., Miller, R., Morcrette, J. J., Myhre, G., Penner, J., Perlwitz, J., Stier, P., Takemura, T., and Zender, C. S.: Global dust model intercomparison in AeroCom phase I, Atmos. Chem. Phys., 11, 7781–7816, doi:10.5194/acp-11-7781-2011, 2011.

Kaufman, Y., Tanre, D., Holben, B., Mattoo, S., Remer, L., Eck, T., Vaughan, J., and Chatenet, B.: Aerosol radiative impact on spectral solar flux at the surface, derived from principal-plane sky measurements, J. Atmos. Sci., 59, 635–646, doi:10.1175/1520-0469(2002)059<0635:ARIOSS>2.0.CO;2, 2002.

Kim, D., Chin, M., Bian, H., Tan, Q., Brown, M. E., Zheng, T., You, R., Diehl, T., Ginoux, P., and Kucsera, T.: The effect of the dynamic surface bareness on dust source function, emission, and distribution, J. Geophys. Res.-Atmos., 118, 871–886, doi:10.1029/2012JD017907, 2013.

Klose, M., Shao, Y., Karremann, M. K., and Fink, A. H.: Sahel dust zone and synoptic background, Geophys. Res. Lett., 37, L09802, doi:10.1029/2010GL042816, 2010.

Knippertz, P.: Dust emissions in the West African heat trough – the role of the diurnal cycle and of extratropical disturbances, Meteorol. Zeitschr., 17, 553–563, 2008.

Knippertz, P. and Todd, M. C.: The central west Saharan dust hot spot and its relation to African easterly waves and extratropical disturbances, J. Geophys. Res.-Atmos., 115, D12117, doi:10.1029/2009JD012819, 2010.

Knippertz, P. and Todd, M. C.: Mineral Dust Aerosols over the Sahara: Meteorological controls on Emission and Transport and Implications for Modeling, Rev. Geophys., 50, RG1007, doi:10.1029/2011RG000362, 2012.

Knippertz, P., Deutscher, C., Kandler, K., Müller, T., Schulz, O., and Schütz, L.: Dust mobilization due to density currents in the Atlas region: Observations from the Saharan Mineral Dust Experiment 2006 field campaign, J. Geophys. Res., 112, doi:10.1029/2007JD008774, 2007.

Kocha, C., Tulet, P., Lafore, J. P., and Flamant, C.: The importance of the diurnal cycle of Aerosol Optical Depth in West Africa, Geophys. Res. Lett., 40, 785–790, doi:10.1002/grl.50143, 2013.

Koch, J. and Renno, N. O.: The role of convective plumes and vortices on the global aerosol budget, Geophys. Res. Lett., 32, L18806, doi:10.1029/2005GL023420, 2005.

Kurosaki, Y. and Mikami, M.: Regional difference in the characteristic of dust event in East Asia: Relationship among dust outbreak, surface wind, and land surface condition, J. Meteorol. Soc. Jpn., 83A, 1–18, doi:10.1029/2003JD003913, 2005.

Kurosaki, Y. and Mikami, M.: Threshold wind speed for dust emission in east Asia and its seasonal variations, J. Geophys. Res.-Atmos., 112, D17202, doi:10.1029/2006JD007988, 2007.

Mahowald, N., Zender, C., Luo, C., Savoie, D., Torres, O., and del Corral, J.: Understanding the 30-year Barbados desert dust record, J. Geophys. Res.-Atmos., 107, 1074, doi:10.1029/2002JD002097, 2002.

Mahowald, N., Bryant, R., del Corral, J., and Steinberger, L.: Ephemeral lakes and desert dust sources, Geophys. Res. Lett., 30, GB4025, doi:10.1029/2002GL016041, 2003.

Mahowald, N., Baker, A., Bergametti, G., Brooks, N., Duce, R., Jickells, T., Kubilay, N., Prospero, J., and Tegen, I.: Atmospheric global dust cycle and iron inputs to the ocean, Global Biogeochem. Cy., 19, GB4025, doi:10.1029/2004GB002402, 2005.

Mahowald, N. M., Ballantine, J. A., Feddema, J., and Ramankutty, N.: Global trends in visibility: implications for dust sources, Atmos. Chem. Phys., 7, 3309–3339, doi:10.5194/acp-7-3309-2007, 2007.

Marsham, J. H., Parker, D. J., Grams, C. M., Taylor, C. M., and Haywood, J. M.: Uplift of Saharan dust south of the intertropical discontinuity, J. Geophys. Res., 113, D21102, doi:10.1029/2008JD009844, 2008.

Marsham, J. H., Knippertz, P., Dixon, N. S., Parker, D. J., and Lister, G. M. S.: The importance of the representation of deep convection for modeled dust-generating winds over West Africa during summer, Geophys. Res. Lett., 38, L16803, doi:10.1029/2011GL048368, 2011.

Marsham, J. H., Hobby, M., Allen, C. J. T., Banks, J. R., Bart, M., Brooks, B. J., Cavazos-Guerra, C., Engelstaedter, S., Gascoyne, M., Lima, A. R., Martins, J. V., McQuaid, J. B., O'Leary, A., Ouchene, B., Ouladichir, A., Parker, D. J., Saci, A., Salah-Ferroudj, M., Todd, M. C., and Washington, R.: Meteorology and dust in the central Sahara: Observations from Fennec supersite-1 during the June 2011 Intensive Observation Period, J. Geophys. Res.-Atmos., 118, 4069–4089, doi:10.1002/jgrd.50211, 2013.

Marticorena, B. and Bergametti, G.: Modeling the Atmosphere Dust Cycle. 1. Design of a Soil-Derived Dust Emission Scheme, J. Geophys. Res.-Atmos., 100, 16415–16430, 1995.

Marticorena, B., Chatenet, B., Rajot, J. L., Traore, S., Coulibaly, M., Diallo, A., Kone, I., Maman, A., Diaye, T. N., and Zakou, A.: Temporal variability of mineral dust concentrations over West Africa: analyses of a pluriannual monitoring from the AMMA Sahelian Dust Transect, Atmos. Chem. Phys., 10, 8899–8915, doi:10.5194/acp-10-8899-2010, 2010.

Mbourou, G., Bertrand, J., and Nicholson, S.: The diurnal and seasonal cycles of wind-borne dust over Africa north of the equator, J. Appl. Meteorol., 36, 868–882, 1997.

McTainsh, G. and Pitblado, J.: Dust Storms and Related Phenomena Measured from Meteorological Records in Australia, Earth Surf. Proc. Landf., 12, 415–424, doi:10.1002/esp.3290120407, 1987.

Middleton, N. J.: A Geography of Dust Storms in Southwest Asia, J. Climatol., 6, 183–196, 1986.

Morales, C.: Saharan Dust, chap. The Use of Meteorological Observations for Studies of the Mobilization, Transport, and Deposition of Saharan Soil Dust, 119–131, John Wiley and Sons, Salisbury, Wiltshire, 1979.

Nicholson, S., Davenport, M., and Malo, A.: A Comparison of the Vegetation response to rainfall in the Sahel and East-Africa, using normalized difference vegetation index from NOAA AVHRR., Clim. Change, 17, 209–241, doi:10.1007/BF00138369, 1990.

Olsson, L., Eklundh, L., and Ardo, J.: A recent greening of the Sahel - Trends, patterns and potential causes, Journal of Arid Environments, 63, 556–566, doi:10.1016/j.jaridenv.2005.03.008, workshop on Changes in the Sahel, Nairobi, Kenya, 14–16 October 2003, 2005.

Ozer, P.: Les lithometeores en region sahelienne, Int. J. Trop. Ecol. Geogr., 24, 9–42, 59–207, 2001.

Parker, D. J., Burton, R. R., Diongue-Niang, A., Ellis, R. J., Felton, M., Taylor, C. M., Thorncroft, C. D., Bessemoulin, P., and Tompkins, A. M.: The diurnal cycle of the West African monsoon circulation, Q. J. Roy. Meteor. Soc., 131, 2839–2860, 2005.

Prospero, J. M.: Environmental characterization of global sources of atmospheric soil dust identified with the NIMBUS 7 Total Ozone Mapping Spectrometer (TOMS) absorbing aerosol product, Rev. Geophys., 40, doi:10.1029/2000RG000095, 2002.

Roderick, M. L., Rotstayn, L. D., Farquhar, G. D., and Hobbins, M. T.: On the attribution of changing pan evaporation, Geophys. Res. Lett., 34, L17403, doi:10.1029/2007GL031166, 2007.

Schepanski, K.: Characterising Saharan Dust Sources and Export using Remote Sensing and Regional Modelling, Ph.D. thesis, 2009.

Schepanski, K., Tegen, I., Todd, M. C., Heinold, B., Bonisch, G., Laurent, B., and Macke, A.: Meteorological processes forcing Saharan dust emission inferred from MSG-SEVIRI observations of subdaily dust source activation and numerical models, J. Geophys. Res.-Atmos., 114, D10201, doi:10.1029/2008JD010325, 2009.

Schepanski, K., Tegen, I., and Macke, A.: Comparison of satellite based observations of Saharan dust source areas, Remote Sens. Environ., 123, 90–97, doi:10.1016/j.rse.2012.03.019, 2012.

Sokolik, I., Winker, D., Bergametti, G., Gillette, D., Carmichael, G., Kaufman, Y., Gomes, L., Schuetz, L., and Penner, J.: Introduction to special section: Outstanding problems in quantifying the radiative impacts of mineral dust, J. Geophys. Res.-Atmos., 106, 18015–18027, doi:10.1029/2000JD900498, 2001.

Spyrou, C., Kallos, G., Mitsakou, C., Athanasiadis, P., Kalogeri, C., and Iacono, M. J.: Modeling the radiative effects of desert dust on weather and regional climate, Atmos. Chem. Phys., 13, 5489–5504, doi:10.5194/acp-13-5489-2013, 2013.

Stocker, T., Qin, D., Plattner, G., Tignor, M., Allen, S., Boschung, J., Nauels, A., Xia, Y., Bex, V., and Midgley, P.: Summary for Policymakers. In: Climate Change 2013: The Physical Science Basis. Contribution of Working Group I to the Fifth Assessment Report of the Intergovernmental Panel on Climate Change, Tech. rep., 2013.

Stensrud, D.: Importance of low-level jets to climate: A review, J. Climate, 9, 1698–1711, 1996.

Sutton, L.: Haboobs, Q. J. Roy. Meteor. Soc., 51, 25–30, 1925.

Tegen, I. and Schepanski, K.: The Global Distribution of Mineral Dust, in: Wmo/Geo Expert Meeting on an International Sand and Dust Storm Warning System, edited by Perez, J. C. and Baldasano, J. M., vol. 7 of IOP Conference Series Earth and Environmental Science, tegen, I. Schepanski, K. WMO/GEO Expert Meeting on an International Sand amd Dust Storm Warning System NOV 07-09, 2007 Barcelona, Spain, 2009.

Todd, M. C., Allen, C. J. T., Bart, M., Bechir, M., Bentefouet, J., Brooks, B. J., Cavazos-Guerra, C., Clovis, T., Deyane, S., Dieh, M., Engelstaedter, S., Flamant, C., Garcia-Carreras, L., Gandega, A., Gascoyne, M., Hobby, M., Kocha, C., Lavaysse, C., Marsham, J. H., Martins, J. V., McQuaid, J. B., Ngamini, J. B., Parker, D. J., Podvin, T., Rocha-Lima, A., Traore, S., Wang, Y., and Washington, R.: Meteorological and dust aerosol conditions over the western Saharan region observed at Fennec Supersite-2 during the intensive observation period in June 2011, J. Geophys. Res.-Atmos., 118, 8426–8447, doi:10.1002/jgrd.50470, 2013.

Tucker, C., Pinzon, J., Brown, M., Slayback, D., Pak, E., Mahoney, R., Vermote, E., and El Saleous, N.: An extended AVHRR 8-km NDVI dataset compatible with MODIS and SPOT vegetation NDVI data, Int. J. Remote Sens., 26, 4485–4498, doi:10.1080/01431160500168686, 2005.

Vautard, R., Cattiaux, J., Yiou, P., Thepaut, J.-N., and Ciais, P.: Northern Hemisphere atmospheric stilling partly attributed to an increase in surface roughness, Nature Geosci., 3, 756–761, doi:10.1038/NGEO979, 2010.

Warner, T. T.: Desert meteorology, Cambridge University Press, 83–91, 2004.

Washington, R. and Todd, M. C.: Atmospheric controls on mineral dust emission from the Bodélé Depression, Chad: The role of the low level jet, Geophys. Res. Lett., 32, L17701, doi:10.1029/2005GL023597, 2005.

Washington, R., Todd, M. C., Engelstaedter, S., Mbainayel, S., and Mitchell, F.: Dust and the low-level circulation over the Bodele Depression, Chad: Observations from BoDEx 2005, J. Geophys. Res.-Atmos., 111, D03201, doi:10.1029/2005JD006502, 2006.

Washington, R., Bouet, C., Cautenet, G., Mackenzie, E., Ashpole, I., Engelstaedter, S., Lizcano, G., Henderson, G. M., Schepanski, K., and Tegen, I.: Dust as a tipping element: The Bodele Depression, Chad, Proc. Natl. Acad. Sci. USA, 106, 20564–20571, 2009.

Williams, E., Nathou, N., Hicks, E., Pontikis, C., Russell, B., Miller, M., and Bartholomew, M. J.: The electrification of dust-lofting gust fronts ("haboobs") in the Sahel, Atmos. Res., 91, 292–298, 2009.

WMO: International Codes-WMO No. 306, Geneva-Switzerland: World Meteorological, 1995.

Zender, C. and Kwon, E.: Regional contrasts in dust emission responses to climate, J. Geophys. Res.-Atmos., 110, D13201, doi:10.1029/2004JD005501, 2005.

Zhu, Z., Bi, J., Pan, Y., Ganguly, S., Anav, A., Xu, L., Samanta, A., Piao, S., Nemani, R. R., and Myneni, R. B.: Global data sets of vegetation leaf area index (LAI) 3g and Fraction of Photosyn-

thetically Active Radiation (FPAR) 3g derived from Global Inventory Modeling and Mapping Studies (GIMMS) Normalized Difference Vegetation Index (NDVI3g) for the period 1981 to 2011, Remote Sens., 5, 927–948, 2013.